ADVANCED SENSOR RESEARCH
Open Access

Supporting Information

Enhanced Broadband Photodetection with Geometry and Interface Engineered Nanocrystalline Graphite

Devang Parmar, Simone Dehm, Naga Anirudh Peyyety, Sandeep Kumar and Ralph Krupke*

Enhanced Broadband Photodetection with Geometry and Interface Engineered Nanocrystalline Graphite

Devang Parmar [*,1,2,3], Simone Dehm [1], Naga Anirudh Peyyety [1], Sandeep Kumar [1], and Ralph Krupke [†,1,2,3]

[1]Institute of Nanotechnology, Karlsruhe Institute of Technology, 76021 Karlsruhe, Germany

[2]Department of Materials Science, Technical University of Darmstadt, 64287 Darmstadt, Germany

[3]Institute of Quantum Materials and Technologies, Karlsruhe Institute of Technology, 76021 Karlsruhe, Germany

Supporting Information

- Finite element method simulation of electric field distribution (Figure S1)

- Gaussian fitting of reflectance data (Figure S2)

- The scanning photocurrent imaging of supported bowtie device (Figure S3)

- The scanning photocurrent imaging of suspended bowtie device (Figure S4)

- Conversion of the supercontinuum spectrum to a smooth power spectrum (Figure S5)

- Laser power dependence of bolometric and PTE currents (Figure S6)

*devang.parmar@kit.edu
†ralph.krupke@kit.edu
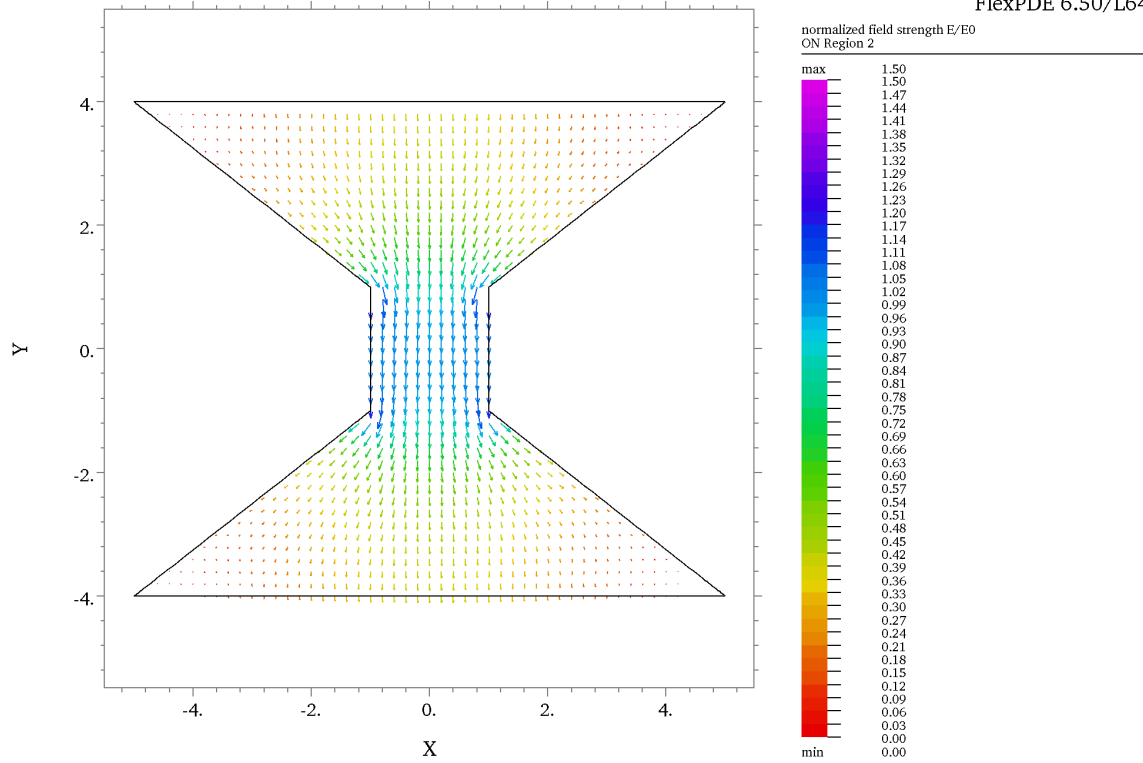
Figure S1: **Finite element method simulation**. Electric field distribution E normalized to E_0 at the center of the NCG constriction ($E_0 = 2 \times 10^4$ V/m @ 100 mV bias). X and Y are in μm and the dimensions and shape match the experiment.
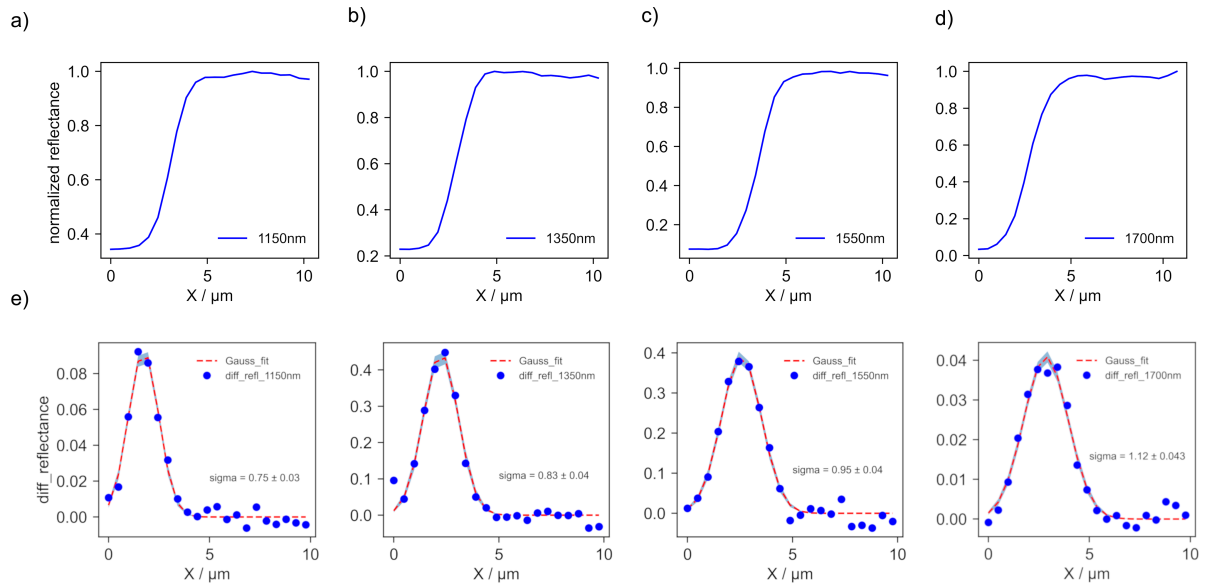
Figure S2: **Gaussian fitting of reflectance data.** a-d) Normalized reflectance signal measured across a reflective edge. e-h) Differentiated reflectance data, fitted to a 1D Gaussian.

For determining the laser beam radius, we have adopted the knife-edge technique[1] by moving the focused laser beam perpendicular to a reflective edge and measuring the reflected power as a function of the beam position. The data in Figure S2a-d shows the reflected laser intensity, normalized to the intensity when completely reflected. Note that for shorter wavelengths the signal does not drop to zero because of reflection from the substrate. Such measurements can be analyzed by fitting the error function

$$F(x) = \frac{1}{2} \cdot (1 + erf(-\frac{x - x_0}{\sqrt{2}\sigma}))$$

to the data. However, it is computationally less demanding and equivalent to fit the 1D Gaussian

$$f(x) = \frac{1}{\sigma\sqrt{2\pi}} exp(-\frac{1}{2}\left(\frac{x - x_0}{\sigma}\right)^2)$$

to the derivative of the data. The results are shown in Figure S2e-h and the sigma values are given. Note that often the beam radius w is defined as the value where the intensity of a Gaussian beam drops to $1/e^2$, and the relation between sigma and w is w = $\sqrt{2}\sigma$.

The sigma values are used to model the laser spot as a radially symmetric Gaussian beam with

a normalized 2D Gaussian function. The fraction of light that falls onto the 2 um x 2um area when positioning the beam at the center of the square is then calculated by integration of the 2D Gaussian across the square area using the code below.

```python
import matplotlib.pyplot as plt
import numpy as np
from scipy.stats import norm
from scipy import integrate
from numba import jit

@jit
def Gauss2D(x,y,xc,yc,sigma):
    g = (1/(sigma*np.sqrt(2*np.pi))**2) * np.exp(-0.5*((x-xc)**2+(y-yc)**2)/sigma**2)
    return g


def Int_Gauss2D(xc,yc,sigma,xw,yw):
    tol = 0.1
    xmin = -7.5; xmax = 7.5
    ymin = -7.5; ymax = 7.5
    f = lambda y, x: Gauss2D(x,y,xc,yc,sigma)
    g_ct = integrate.dblquad(f, -xw/2, xw/2, -yw/2, yw/2, epsabs=tol, epsrel=tol)
    return g_ct[0]

xw=2; yw=2 # square area over which 2D Gaussian is integrated
sigma = 0.95 # sigma value extracted from Gaussian fitting in Figure S2
fraction = Int_Gauss2D(0,0,sigma,xw,yw) # fraction of total intensity that is falling onto the square area (2umx2um)
print (fraction)
```

0.5005422724673806

The table below lists the sigma values extracted from the Gaussian fitting in Figure S2, the fraction of the total intensity that falls onto the square as calculated from the code above, the total power of the light source, and the power that falls onto the square area of the constriction.

wavelength/nm	sigma/um	fraction	total power	fractional power
1150	0.75 ± 0.03	66.8%	220uW	147uW
1350	0.83 ± 0.04	59.6%	565uW	336uW
1550	0.95 ± 0.04	50.0%	673uW	337uW
1700	1.12 ± 0.04	39.5%	694uW	274uW
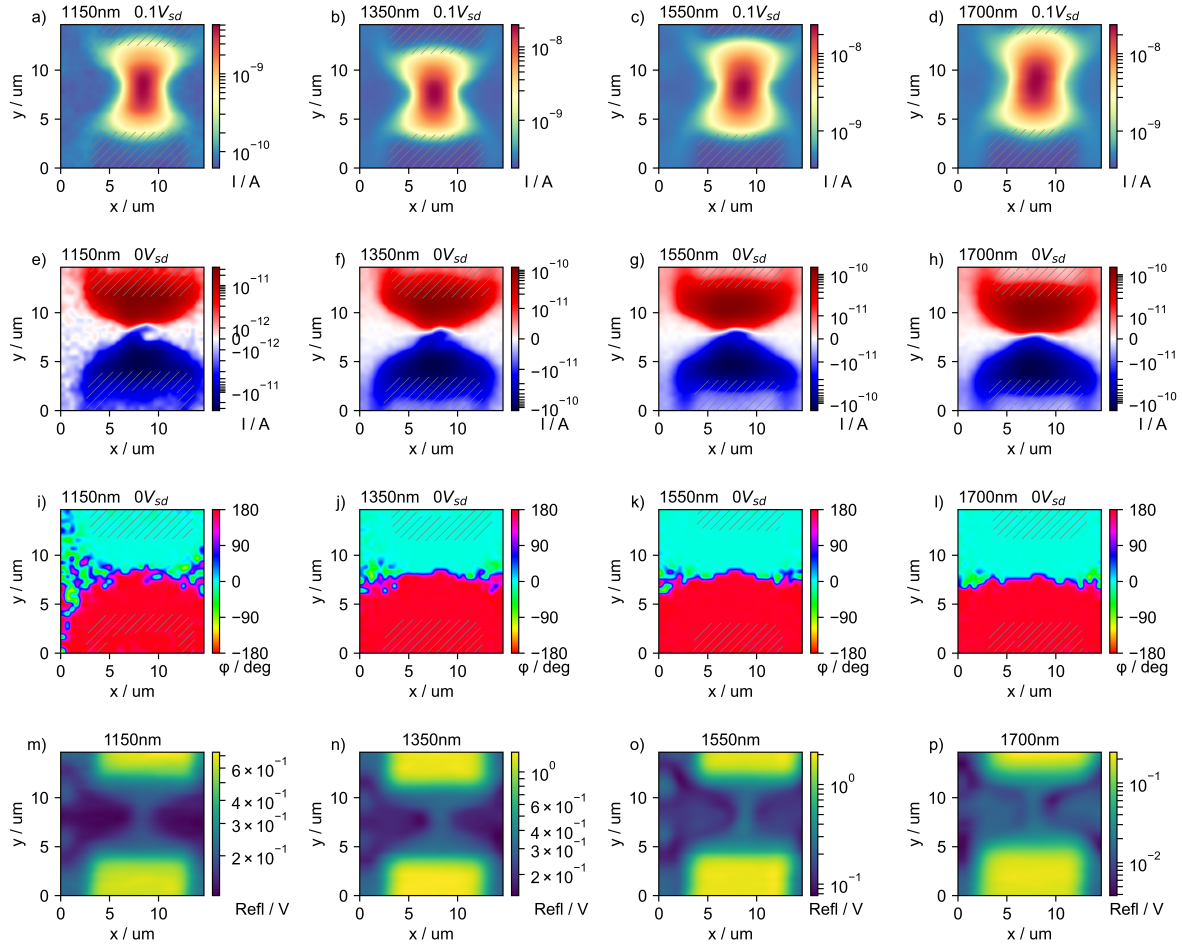
Figure S3: **Scanning photocurrent imaging of a substrate-supported constriction device.** Data is shown for the wavelengths 1150nm, 1350nm, 1550nm and 1700nm: (a-d) In-phase photocurrent maps measured at 0.1V bias. (e-h) Zero-bias in-phase photocurrent maps with corresponding phase maps shown in (i-l). (m-p) Reflectance signal, plotted on logarithmic scale. The reflectance signal from the electrodes is overlaid as gray-shaded areas to the maps a-l. Data is identical to Figure 3, but the photocurrent maps are plotted on logarithmic scale.
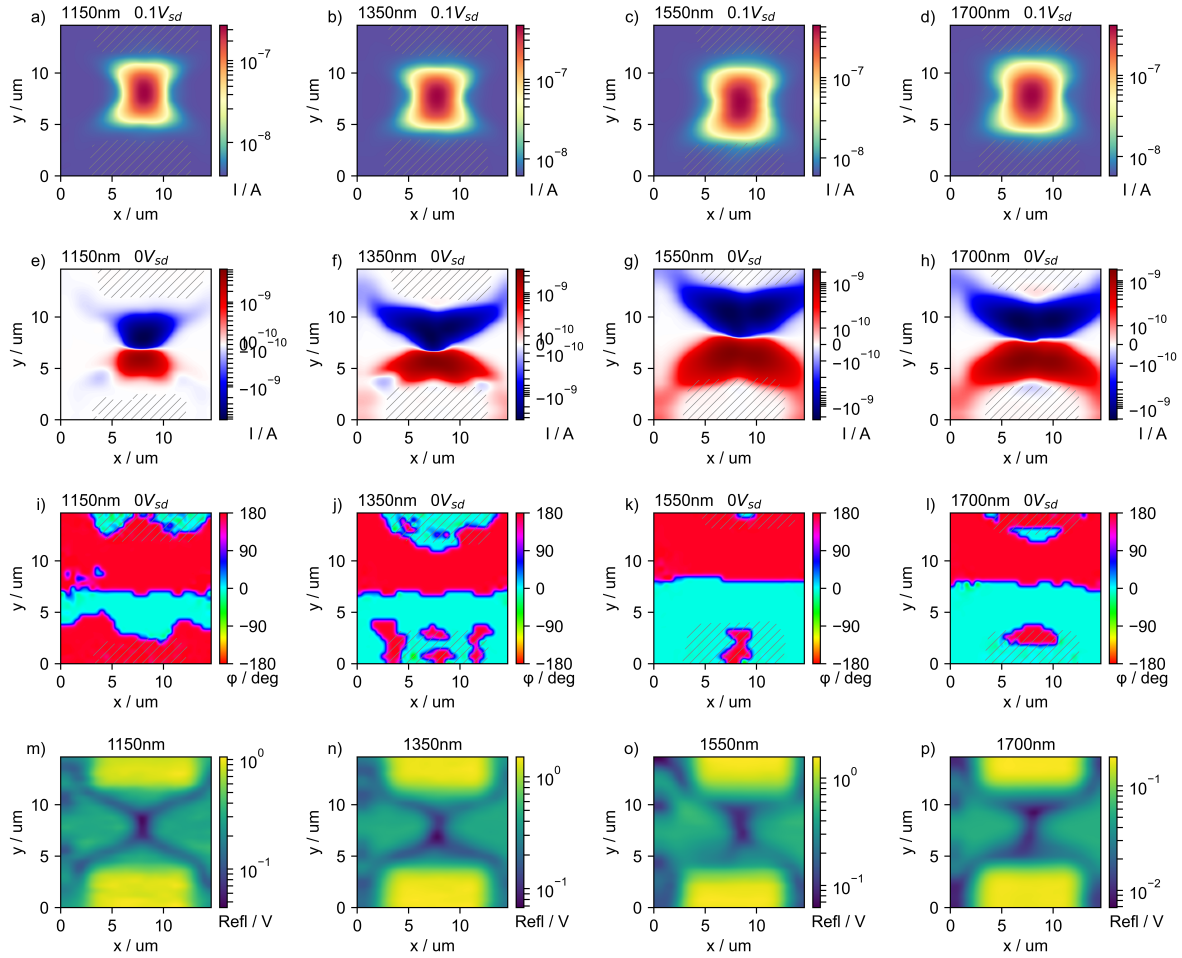
Figure S4: **Scanning photocurrent imaging of a suspended constriction device.** Data is shown for the wavelengths 1150nm, 1350nm, 1550nm and 1700nm: (a-d) In-phase photocurrent maps measured at 0.1V bias. (e-h) Zero-bias in-phase photocurrent maps with corresponding phase maps shown in (i-l). (m-p) Reflectance signal, plotted on logarithmic scale. The reflectance signal from the electrodes is overlaid as gray-shaded areas to the maps a-l. Data is identical to Figure 4, but the photocurrent maps are plotted on logarithmic scale.
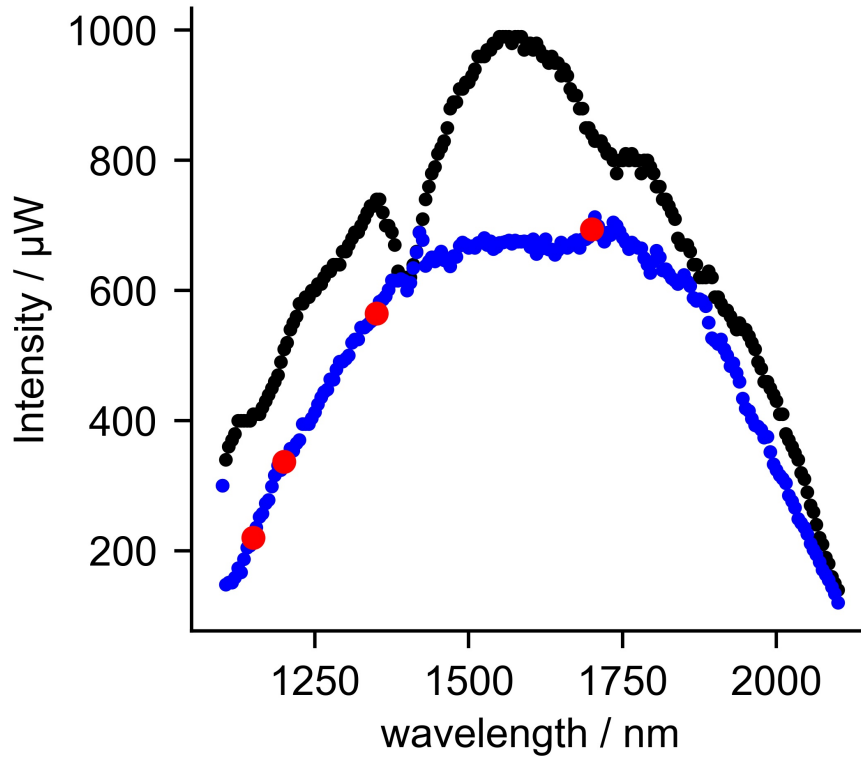
Figure S5: **Conversion of the supercontinuum spectrum to a smooth power spectrum.** A wavelength-specific intensity modification to the acousto-optic tunable filter (AOTF) transforms the supercontinuum (SC) spectrum(black) to a smooth power spectrum(blue). The highlighted red wavelengths are used in the measurement (1150nm, 1350nm, 1550nm, and 1700nm).
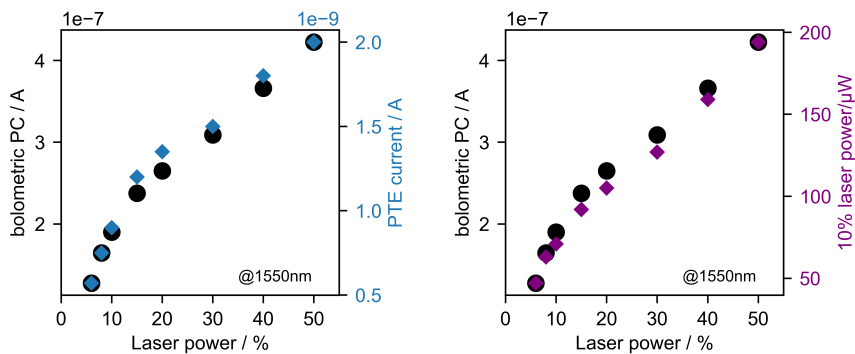
Figure S6: **bolometric and thermoelectric photocurrent at different laser power.** Left: Comparison of bolometric and PTE currents, both plotted versus the nominal laser power. Right: Comparison of bolometric photocurrent and laser power measured at the 10% beam-splitter output, both plotted versus the nominal laser power. Bolometric and PTE currents depend linear on laser power above 10% of the maximum laser power. Below 10%, the real laser output does not correspond to the nominal setting because of non-linearities at low laser excitation power and a threshold of emission at around 5%.

References

[1] de Araújo, M. A.; Silva, R.; de Lima, E.; Pereira, D. P.; de Oliveira, P. C. *Applied optics* **2009**, *48*, 393–396.